Polymer Chemistry

Accepted Manuscript

ROYAL SOCIETY OF CHEMISTRY

www.rsc.org/polymers

Strong Emission of 2,4,6-Triphenylpyridine-Functinalized Polytyrosine and Hydrogen-Bonding Interactions with Poly(4-vinylpyridine)

Mohamed Gamal Mohamed,[a] Fang-Hsien Lu,[a] Jin-Long Hong[a] and Shiao-Wei Kuo[a,b,c*]

Received (in XXX, XXX) Xth XXXXXXXXX 200X, Accepted Xth XXXXXXXXX 200X
First published on the web Xth XXXXXXXXX 200X
DOI: 10.1039/b000000x

In this paper, 2,4,6-triphenyl pyridine-functionalized polytyrosine (Pyridine-PTyr) was successfully synthesized by living ring-opening polymerization where 2,6-bis(4-aminophenyl)-4-phenylpyridine (Pyridine-NH_2) was an initiator. The photo-physical characteristics of Pyridine-NH_2 and Pyridine-PTyr was elucidated via UV-Vis absorption and photoluminescence spectra, revealing that unlike Pyridine-PTyr, Pyridine-NH_2 shows solvatochromic effects in solvents of different polarities. Additionally, Pyridine-NH_2 exhibited aggregation-caused quenching (ACQ) phenomena; however, it became an aggregation-induced emission (AIE) material after attachment to the rigid-rod conformation of polytyrosine. Based on differential scanning calorimetry results, we observed that after blending Pyridine-PTyr with P4VP revealed a single glass transition temperature due to their miscibility through intermolecular hydrogen bonding of phenolic OH groups in PTyr backbone and pyridine ring in P4VP as indicated by IR spectroscopy. Obviously, the emission intensity of Pyridine-PTyr was decreased after blending with P4VP and hypsochromic shift from 536 to 489 nm, presumably due to the release of the restricted intramolecular rotation of triphenyl pyridine unit in the center of the polymer and the polymer chain of Pyridine-PTyr becomes separated random coils based on WAXD results.

Introduction

Polypeptides are a class of amino acid-based polymers, which have been received much attention many researchers in the recent years because of their potential applications as biocompatible materials and conformational transitions.[1-6] It is well established that there are three kinds of secondary structure of polypeptides in both solution and bulk state, including α-helical, β-sheets and random coil.[7-8] The secondary structures of polypeptide is dependent on degree of polymerization. Such as, if the degree of polymerization is higher than 18; the secondary structures of polypeptide will be α-helical structure which can be act as rigid-rod like polymers and it is stabilized through intramolecular hydrogen bonding interaction.[9] The synthetic polypeptide is carried out via living-ring opening polymerization of N-carboxyanhydride [NCA] of versatile peptide monomers derivatives at room temperature with controlled polydispersity index (PDI).[10-11] Much literature reported that the introduction of carbohydrates[12-13] and poly(ethylene oxide)[14-15] in main or side chain of polypeptide backbone, these smart materials can behave as drug delivery and stimuli-responsive polymers.

Recently, the non-covalent interaction plays a crucial role to form supramolecular complexes without any chemical reaction. The non-covalent interactions are including hydrophobic interaction, dipole-dipole interaction, metal-ligand coordination and hydrogen bonding interaction. In this report, we employed hydrogen bonding interaction as one of the best useful method to form supramolecular complexes because of its moderate strength and reversibility.[19] In addition to the addition of functional moieties into the main chain or a side chain of polypeptides, the polymers is another convenient method for improving the thermal or self-assembly behavior of polypeptides.[16-18] For example, we concluded the blending of poly(γ-benzyl-L-glutamate) (PBLG) with random-coil oligomers through intermolecular hydrogen bonding to hydrogen bond donor polymers, the secondary blending with other structures of PBLG were altered.[19,20] Also, we demonstrated that the chain behavior of PTyr/P4VP blend through intermolecular hydrogen bonding in MeOH, and DMF solution. The chain behavior of PTyr/P4VP was turned to inter-polymer complex aggregates and separated random coil based on FTIR spectroscopy and wide-angle X-ray diffraction analyses.[21]

Fluorescent-organic materials have been designed and attracting materials in the recent years due to their interesting optical potential applications in optoelectronic devices[22] and as fluorescence sensors[23-24] However, the emission of most organic fluorescent materials (pyrene, carbazolyl, dansyl) become weak or non-emissive materials at high concentration or in aggregated state due to their strong intermolecular π-π interaction;[25] this effect is known as aggregation-caused quenching (ACQ). This effect results in an increased possibility of π-π stacking leading to formation of excimers and exciplexes in the excited state.[26] Therefore, to solve this problem, it is important to develop new fluorescent materials that emit more efficiently in solid and an aggregate state than as monomers in solution. Such materials are associated with two unusual phenomena that are exact opposites of the ACQ and were identified by Tang et al.[27] Aggregation-induced emission (AIE)/aggregation-induced enhancement emission (AIEE) luminescent materials are weak or non-luminescent in solution state, but these materials become strong emissive when their aggregated as nanoparticles in solution and condensed state. These researchers reported the first aggregation-induced emission (AIE) active compounds based on the pentaphenyl derivatives of silole that showed only a weak fluorescence in solution and were highly fluorescence after aggregation. These authors also reported that the mechanism of aggregation-induced emission is associated with the restriction of intramolecular rotation (RIR) of the fluorophore compound.[27] Additionally, Hong et al. reported AIE material's attachment to polypeptide through covalent chemical bonding and ionic interactions.[28] For example, Hong et al. designed two kinds of PBLG as TP1PBLG and TP2PBLG containing

[a]Department of Materials and Optoelectronic Science, National Sun Yat-Sen University, Kaohsiung, Taiwan.
[b]Department of Medicinal and Applied Chemistry, Kaohsiung Medical University, Kaohsiung, Taiwan.
[c]School of Chemical Engineering, East China University of Science and Technology, Shanghai, China
E-mail:kuosw@faculty.nsysu.edu.tw

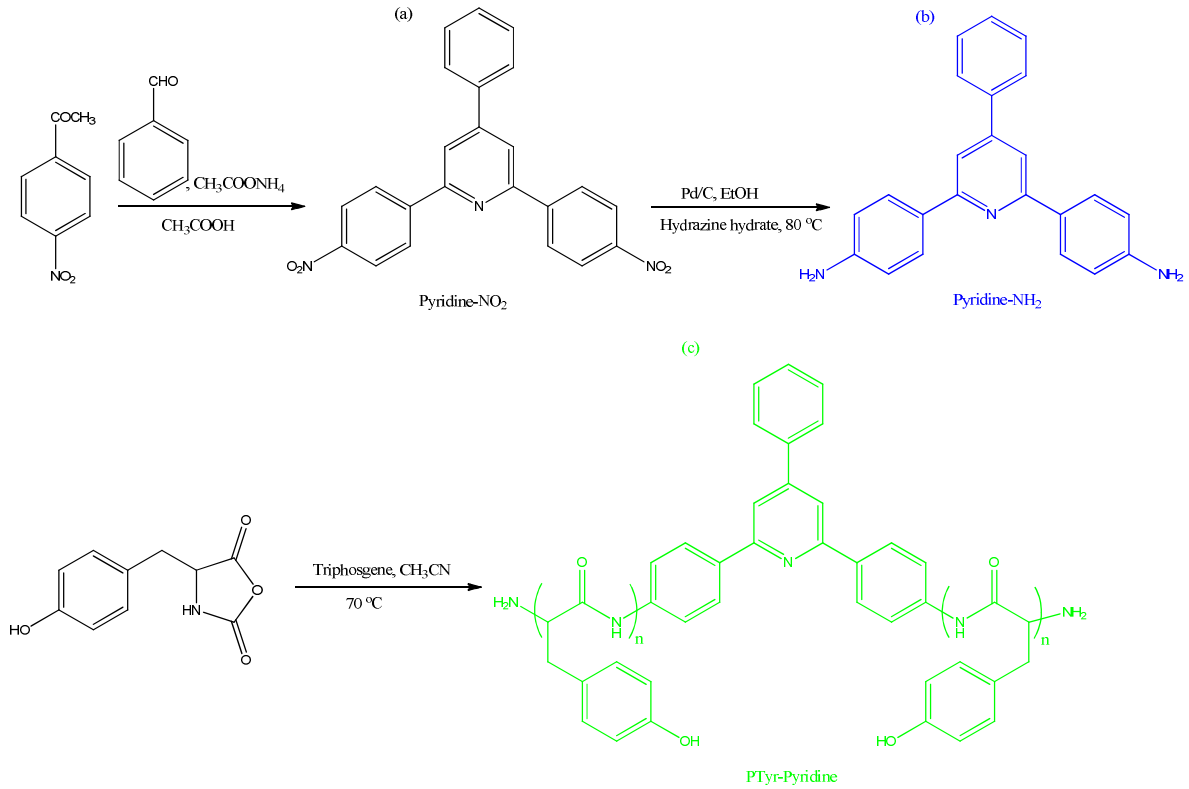

Scheme 1: Synthesis of (a) Pyridine-NO_2, (b) Pyridine-NH_2, and (c) Pyridine-PTyr

tetraphenylthiophene (TP) with aggregation-induced emission property. These researchers found that the emission intensity of TP unit in TP2PBLG was decreased due to the intermolecular aggregate of the central TP unit in the TP2PBLG is sterically blocked by the large α-helical PBLG chains, leading to the reduced AIEE.[28] Recently, they also reported that (E)-4-(2-(anthracen-9-yl)vinylpyridine (AnPy) blended with different amounts of polytyrosine through hydrogen bond interactions exhibits intramolecular charge transfer (ICT) and AIE properties at a low AnPy content.[29] Building on the studies described above, in this work, we successfully synthesized 2,6-bis(4-aminophenyl)-4-phenylpyridine (Pyridine-NH_2) as initiator for living ring-opening polymerization of L-tyrosine-N-carboxyanhydride (NCA) to obtain Pyridine-PTyr (Scheme 1). We used photoluminescence spectroscopy to investigate the fluorescence characteristics of Pyridine-NH_2 and Pyridine-PTyr. We expected that Pyridine-PTyr, possessing phenolic OH groups, will form intermolecular hydrogen bonds with poly(4-vinylpyridine) (P4VP) and may exhibit separated coil behavior in this polymer blend in N-dimethylformamide (DMF) solution. We used differential scanning calorimetry (DSC), Fourier transform infrared (FTIR) spectroscopy, UV-Vis spectroscopy, and photoluminescence spectroscopy to investigate the miscibility behavior, hydrogen bonding interactions and secondary structures of PTyr-Pyridine/P4VP blends.

Experimental Section

Materials

Benzaldehyde, p-nitroacetophenone, ammonium acetate, and 10 wt% Pd/C (Merck) were used as received. DMF, ethanol and methanol were purchased from Merck and dried over calcium hydride overnight, distilled under reduced pressure. L-Tyrosine was purchased from MP Biomedicals. Triphosgene (TCI), P4VP (Aldrich, 160,000 g/mol), MeCN (Across, 99.5%), hexane (Across), MeOH (Across), dichlorormethane (DCM), dimethylsulfoxide (DMSO), acetone, and Tetrahedrofuran (THF) were purchased from Tedia. L-Tyrosine N-carboxyanhydride (Tyr-NCA) was prepared according to our previous study[21] and synthesis of Pyridine-NO_2 has been reported previously.[30]

Synthesis of 2,6-bis(4-aminophenyl)-4-phenylpyridine (Pyridine-NH_2)[30]

A mixture of Pyridine-NO_2 (2.500 g, 0.012 mol), 0.075 g of 10% Pd/C were dissolved in 60 mL of anhydrous ethanol. Then, the reaction mixture was heated to 90 °C for 3 h in 150-mL two neck bottomed flask equipped with a stirring bar under N_2 atmosphere. After that, added dropwise of 20 mL of hydrazine monohydrate (in 20 mL of ethanol). The reaction mixture was heated to 80 °C overnight and then subsequently filtered to remove the Pd/C. After cooling to room temperature, the yellow solid crystals were isolated by filtration, twice recrystallized from ethanol, and vacuum-dried to obtain the product (1.50 g, 70%) that exhibits a melting point of 201 °C (DSC, Figure S1). The following peaks of the FTIR (KBr, cm^{-1}) spectrum were obtained: 3471 and 3379 cm^{-1} (N-H stretching), and 1620 cm^{-1} (N-H deformation). ^{1}H NMR obtained chemical shifts of (500 MHz, DMSO-d_6, δ, ppm): 6.71-8.04 (14H, Aromatic protons), and 5.42 (4H, NH_2) (Figure S2). The following chemical shifts were observed for ^{13}C NMR (125 MHz, DMSO-d_6, δ, ppm): 156.63, 149.89, 148.66, 138.59, 129.025, 127.79, 127.082, 126.59, 113.70, 112.74. High resolution FT-MS $[M+H]^+$ m/z for ($C_{23}H_{19}N_3$): 338.17: calc.: 337.42 (Figure S3).

Synthesis of Pyridine-PTyr by ring opening polymerization (ROP) of Tyr-NCA

Tyr-NCA (3.00 g, 11.34 mmol) was weighted in a dry box under N_2, placed in three-neck bottle, and dissolved in anhydrous DMF (20 mL). The solution mixture was stirred for 15 min prior to the

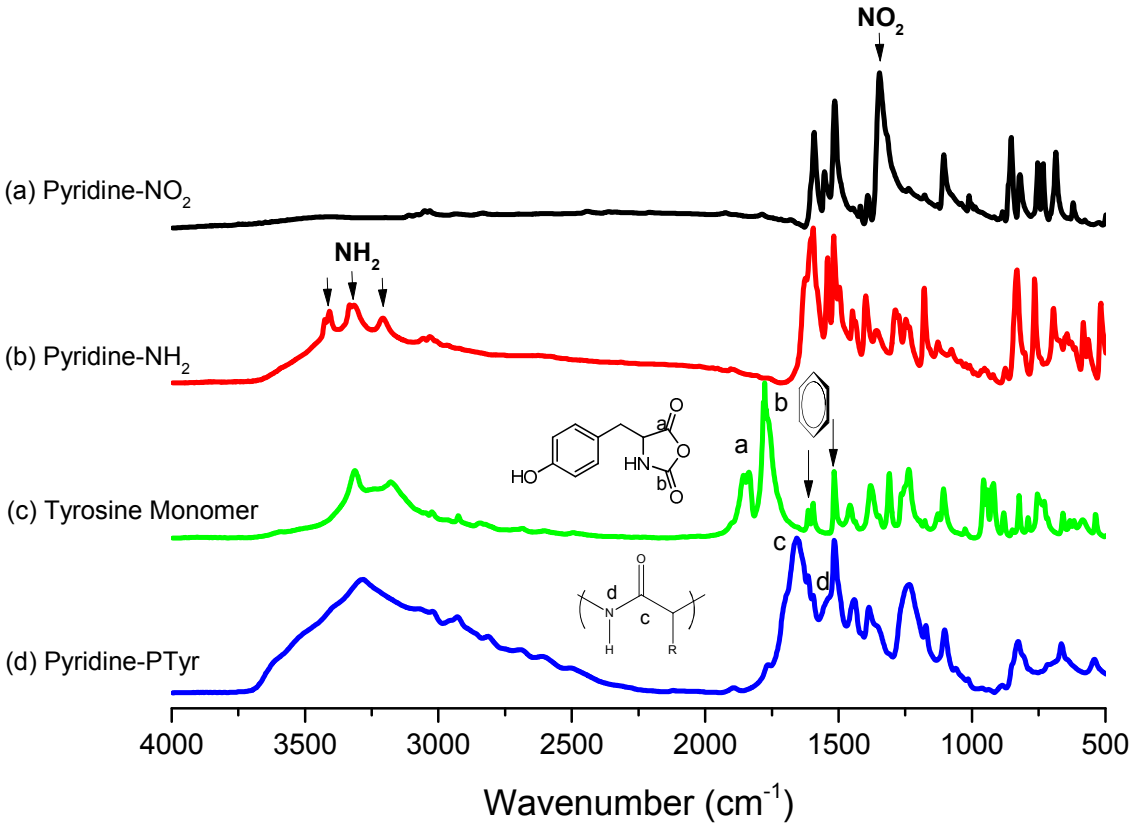

Figure 1: FTIR spectra of (a) Pyridine-NO_2, (b) Pyridine-NH_2, (c) Tyrosine nonomer, and (d) Pyridine-PTyr, recorded at room temperature.

introduction of a solution of Pyridine-NH_2 (0.08 g, 0.23 mmol) in anhydrous DMF (3 mL) using a nitrogen purged syringe. After stirring for 72 h at 0 °C, the polymer was recovered through precipitation in diethyl ether (Et_2O) and was subsequently dissolved in methanol and recovered through precipitation in ether. The polymer was purified three times from methanol/ether to give a pure yellow powder and was dried under high vacuum at 30 °C. A yield of 2.5 g was obtained. The following peaks were obtained in FTIR (KBr, cm^{-1}) spectra: 3288 (NH), 1601, 1590, 753, 698 (Ar). ^{1}H NMR chemical shifts were (500 MHz, DMSO-d6, δ, ppm): 2.90 (d, 2H, CH_2), 4.40 (t, 1H), 6.69 (d, 2H, Ar), 6.95 (d, 2H, Ar), 7.94 (s, 1H, NH) 9.14 (s, 1H). M_n = 11768 g/mol, PDI = 1.22 (GPC, Figure S4).

The Preparation of Pyridine-PTyr with P4VP Blending

Mixtures of Pyridine-PTyr/P4VP were prepared by dissolving various weight percent of P4VP with Pyridine-Ptyr in DMF solution; the solutions were then stirred for 2 days to generate intermolecular hydrogen bonding interactions. The solvent was then evaporated in high vacuum at 60 °C for 72 h.

Characterization

^{1}H and ^{13}C nuclear magnetic resonance (NMR) spectra were obtained using an INOVA 500 instrument with DMSO-d_6 as *d*-solvents and tetramethylsilane (TMS) as the external standard. FTIR spectra were recorded using a Bruker Tensor 27 FTIR spectrophotometer and the conventional KBr disk method; 32 scans were collected at a spectral resolution of 4 cm^{-1}. The films used in this study were sufficiently thin to obey the Beer–Lambert law. Mass spectra were obtained using a Bruker Daltonics Autoflex MALDI-TOF mass spectrometer. The following voltage parameters were used: ion source 1, 19.06 kV; ion source 2, 16.61 kV; lens, 8.78 kV; reflector 1, 21.08 kV; reflector 2, 9.73 kV. The molecular weight of Pyridine-NH_2 was recorded using a Bruker Solarix high resolution Fourier Transform Mass spectroscopy system FT-MS (Bruker, Bremen, Germany. Molecular weight and molecular distributions of Pyridine-PTyr were determined through gel permeation chromatography (GPC) using a waters 510 high performance liquid chromatograph (HPLC) equipped with a 410 differential refractometer and three ultrastragel columns (500, 580, and 10 Å) connected in series, with DMF as the eluent (flow rate: 0.4 mL min^{-1}). DSC analyses were performed using TA Q-20 differential scanning calorimeter operated under N_2 atmosphere. The sample (ca. 5-7 mg) was placed in a sealed aluminum sample pan and heated from 25 to 200 °C at a heating rate of 20 °C/min. A wide-angle X-ray diffraction (WAXD) pattern was obtained from the wiggler beamline BL17A1 of the National Synchrotron Radiation Research Center (NSRRC), Taiwan. A triangular bent Si (111) single crystal was used to obtain a monochromated beam with a wavelength (λ) of 1.33 Å. The samples were annealed at 180 °C for 2 h, and then cooled to room temperature before measurement WAXD. UV–Vis absorption spectra were recorded with an ocean optics DT 1000 CE 376 spectrophotometer. A small quartz cell with dimensions of 0.2 × 1.0 × 4.5 cm^3 was used to accommodate the solution sample and the concentration of samples in organic solvent was 10^{-4} M. PL was obtained from a LabGuide X350 fluorescence spectrometer using a 450 w Xe lamp as the continuous light source. Quantum yields (Φ_f) of the Pyridine-NH_2 and Pyridine-PTyr solutions were determined by using a quinine sulfate as a standard solution and quantum efficiency (Φ_f) of the solid samples and polymer blends (Pyridine-PTyr/P4VP) were measured in an integrated sphere by ocean optics. Fluorescence

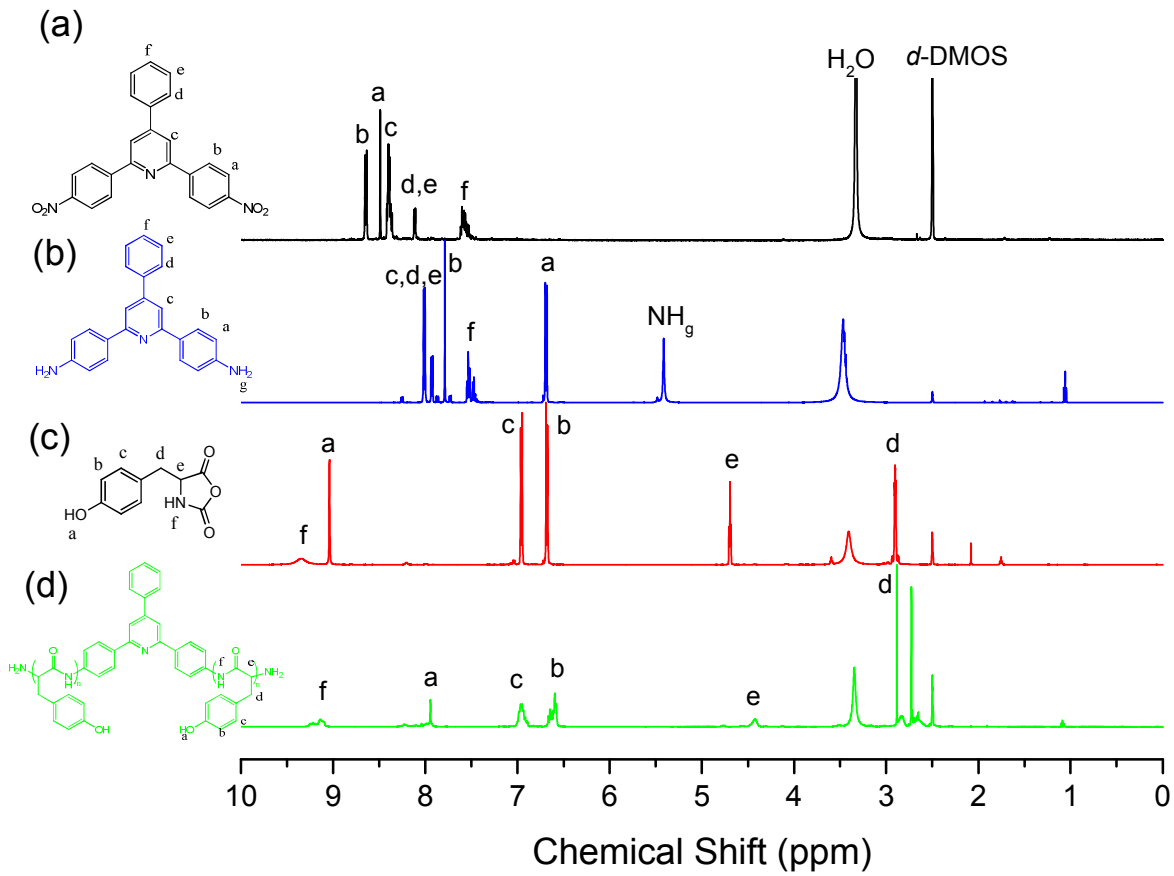

Figure 2: ^{1}H NMR spectra of (a) Pyridine-NO_2, (b) Pyridine-NH_2, and (c) Tyrosine monomer and (d) Pyridine-PTyr.

lifetime measurement was performed by HITACHI F-4500 Fluorescence Spectrometers with a light source of 150W XENON lamp. The PL lifetime of solid state Pyridine-NH_2 and Pyridine-PTyr were measured at emitting bands at 500 nm with exciting wavelength 350 nm).

Results and Discussion

Pyridine-NH_2 Synthesis

Scheme 1 shows the synthesis of the diamine compound containing a pyridine heterocyclic ring, 2,6-bis(4-aminophenyl)-4-phenyl pyridine (Pyridine-NH_2). The dinitro compound containing a pyridine heterocyclic ring (Pyridine-NO_2) was prepared through a facile Chichibabin reaction.[31] The condensation of benzaldehyde with p-nitroacetophenone in the presence of ammonium acetate at reflux in glacial acetic acid obtained the dinitro-containing pyridine.[30] Next, reduction of pyridine dinitro in the absolute ethanol with hydrazine monohydrate in the presence of catalytic amount of palladium on activated carbon at 80 ^{o}C was used to obtain the diamine compound (Pyridine-NH_2). Both FTIR and NMR spectroscopies and confirmed the structure of these compounds. Figures 1(a) and 1(b) show the FTIR spectra of Pyridine-NO_2 and Pyridine-NH_2, respectively. We can clearly observe the signals at 1525, and 1345 cm^{-1} due to the NO_2 group, while the signals at 3472 and 3379 cm^{-1} are due to NH stretching vibrations in Pyridine-NH_2 compound. Based on proton NMR spectra in Figures 2 (a) and 2 (b) indicated that the formation of pyridine heterocyclic group as deduced from the chemical shifts at 7.99 ppm for diamine compound and a new signals appeared in the ^{1}H-NMR spectra at 5.40 ppm due to the amino group. Additionally, Figures 3(a) and 3(b) present the ^{13}C-NMR spectra of Pyridine-NO_2 and Pyridine-NH_2, respectively. The carbon resonance signal of C2 in Pyridine-NO_2 appeared at 119.00 ppm, while the signal of the carbon resonance of C2 in Pyridine-NH_2 was shifted to 115.20 ppm. A FT-MS spectrum displays the molecular weight $[M+H]^{+}$ for Pyridine-NH_2, which is consistent with the predicted molecular weight as shown in Figure S3. These results confirm that we obtained a highly pure diamine compound that contains pyridine (Pyridine-NH_2).

Synthesis of Pyridine-PTyr by Ring Opening Polymerization (ROP) of Tyr-NCA

Pyridine-PTyr was easily prepared via the diamine containing a pyridine heterocyclic ring initiated ring-opening polymerization (ROP) of L-Tyrosine N-carboxyanhydride at room temperature.[32] Figures 1(c) and 1 (d) present the FTIR spectra of the Tyr-NCA monomer and the Pyridine-PTyr polymer. FTIR spectroscopy showed the characteristic anhydride peaks at (a) 1850 and (b) 1772 cm^{-1}, which assigned to the two typical C=O stretching vibrations in the Tyr-NCA monomer. Using Pyridine-NH_2 as the initiator, the ring-opening polymerization of Tyr-NCA was performed in DMF as solvent at room temperature for 72 h. After ROP of the NCA monomer, the FTIR spectra as depicted in Figure 1(d) revealed the appearance of characteristics absorption peaks for due to the peptide bands in the polymer backbone at 1652, 1626 (c), and 1531 (d) cm^{-1}.[21] Figure 2(c) shows the ^{1}H-NMR spectrum of the Tyr-NCA monomer in

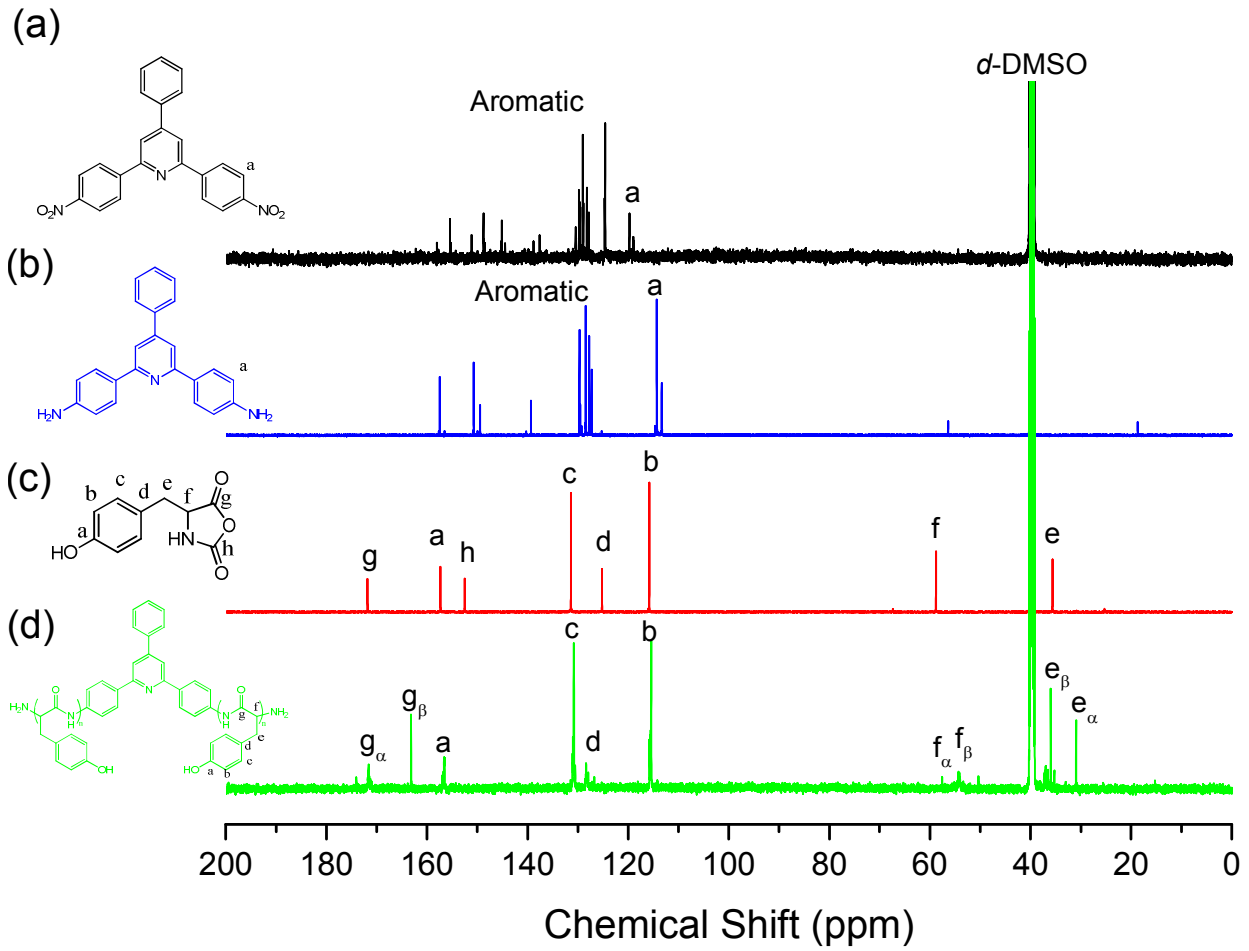

Figure 3: ^{13}C NMR spectra of (a) Pyridine-NO_2, (b) Pyridine-NH_2, and (c) Tyrosine monomer and (d) Pyridine-PTyr.

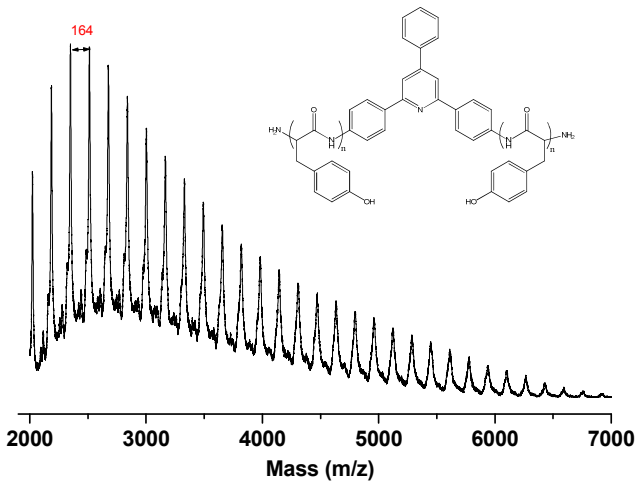

Figure 4: MALDI-TOF mass spectrum of Pyridine-PTyr

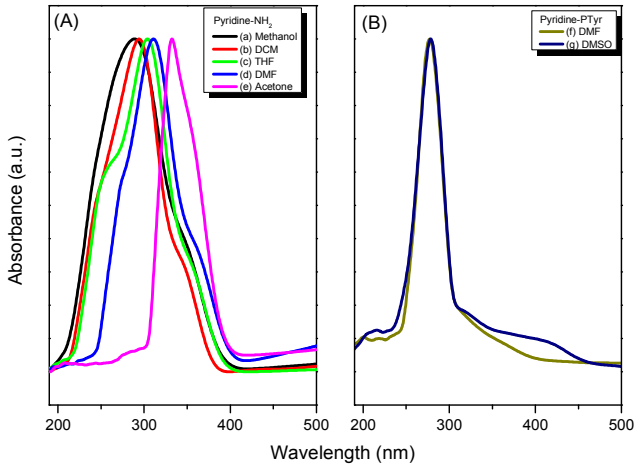

Figure 5: UV-Vis absorption spectra of (A) Pyridine-NH_2, and (B) Pyridine-PTyr at concentration of 10^{-4} M.

DMSO-d_6. The singlet of proton on the nitrogen atom (NH) and OH group appeared at 9.34, 9.04 ppm, respectively. The resulting Pyridine-PTyr was analyzed via ^{1}H NMR spectrum in Figure 2(d) clearly shows the characteristic peaks signal of proton NH (8.05 ppm), phenolic OH protons (9.24 ppm), backbone COCHNH (4.66 ppm), and CH_2 protons (2.49 ppm). Figure 3 (c) presents the ^{13}C-NMR spectrum of the tyrosine monomer in DMSO-d_6. The characteristic signals of the C=O carbon atoms (172.54, 152.02), the phenolic C-OH carbon atoms (154.44 ppm), and the benzyl carbon atom and the amino acid α-carbon atoms (NHCOC) (35.05, 58.88 ppm) of the tyrosine monomer. Figure 3(d) displays the ^{13}C-NMR spectrum of the Pyridine-PTyr in DMSO-d_6,

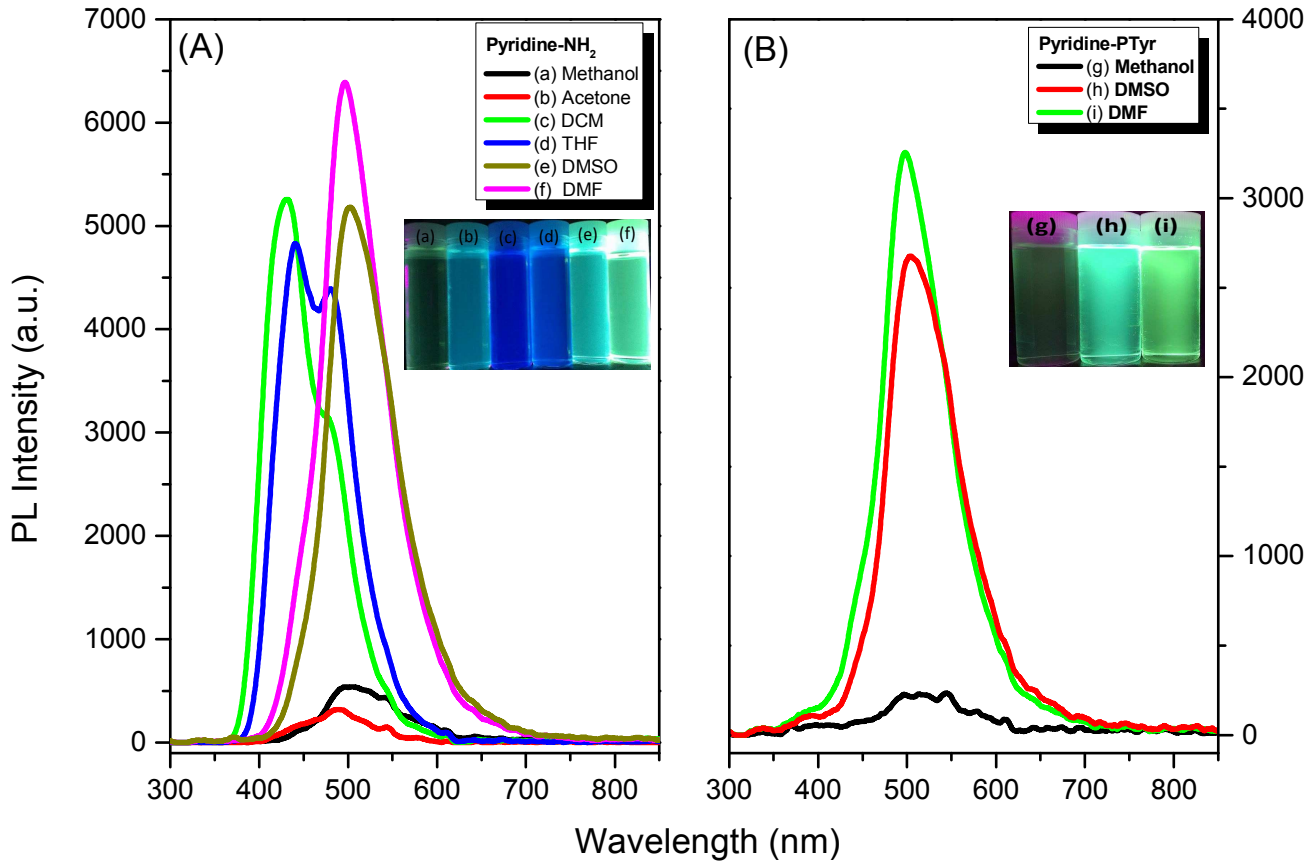

Figure 6: Photoluminescence spectra of (A) Pyridine-NH_2 and (B) Pyridine-PTyr at concentration of 10^{-4} M.

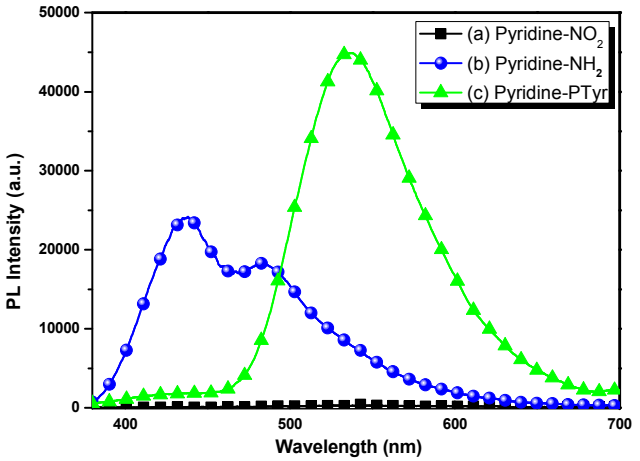

Figure 7: Photoluminescence spectra of (A) Pyridine-NO_2, (B) Pyridine-NH_2, and (C) Pyridine-PTyr in solid state with excitation wavelength (350 nm).

revealing that the C=O and amide carbon atoms signals appeared in the Pyridine-PTyr at 171 and 162.6 ppm, respectively. The chemical shift at 55.65 ppm is ascribed the amino acid α-carbon atoms. Figure 4 presents the MALDI-TOF mass spectrum of Pyridine-PTyr. Clearly, the mass difference between all adjacent peaks for Pyridine-PTyr is *m/z* 164 for a tyrosine repeating unit. Together, our results for ^{1}H, ^{13}C-NMR, FTIR spectroscopic analyses and MALDI-TOF mass spectrum confirmed the successful synthesis of Pyridine-PTyr (M_n = 3416 Da, PDI = 1.10).

Solvent Effect of Pyridine-NH_2 and Pyridine-PTyr

Initially, to elucidate the solvatochromism effect, the photophysical properties of Pyridine-NH_2 and PTyr-Pyridine were investigated by absorption and emission spectroscopy at ambient temperature in different polar solvents. Pyridine-NH_2 exhibited good solubility in methanol, dichloromethane, acetone, THF, DMF and DMSO, while PTyr-Pyridine was soluble in methanol, DMF and DMSO and insoluble in acetone, DCM and THF. As depicted in Figure 5(A), the Pyridine-NH_2 absorption spectra indicate that the absorption band was varied depending on the nature of solvent; this effect can be assigned to the π-π* transition. For example, Pyridine-NH_2 showed the absorption band at 290 nm in methanol, 292 nm in dichloromethane, 303 nm in DMF, and 310 nm in DMSO. The absorption band of Pyridine-NH_2 was red shifted to 333 nm in acetone due to strong guest-host interaction between the molecule and acetone environment. On the other hand, the absorption peak of Pyridine-NH_2 in methanol shifted to lower wavelength because may be the fluorophore in ground state is more stabilized compared to excited state and may lead to form complex with less length conjugation. The absorption behaviour of Pyridine-NH_2 monomer is strongly dependent on solvent polarity.[26]

Figure 5(B) represents the absorption spectra of Pyridine-PTyr in DMF and DMSO. The high energy band (277 nm) has been assigned as π-π* transition that is attributed to the phenyl group in tyrosine and triphenyl pyridine unit in both DMF and DMSO, respectively. To obtain further insight in the characteristics of the emissions from Pyridine-NH_2 and Pyridine-PTyr, it is necessary to do a series of experiments in solution and solid states. Figure 6(A) presents the Pyridine-NH_2 fluorescence emission spectra measured in solvents of different polarities, such

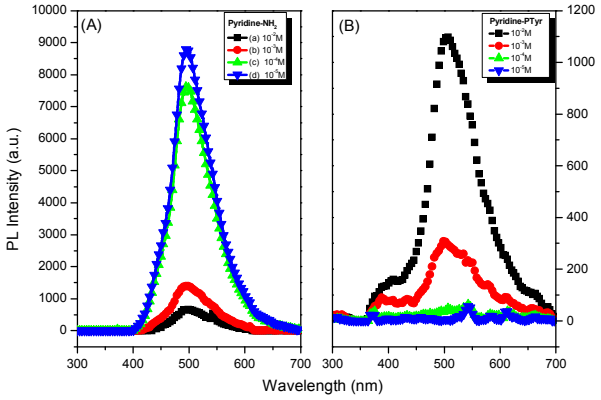

Figure 8: Photoluminescence spectra of (A) Pyridine-NH_2 (DMF) and (B) Pyridine-PTyr (Methanol) with excitation wavelength (350 nm)

as methanol, acetone, DCM, THF, DMSO, DMF. Interestingly, Pyridine-NH_2 shows emission peaks at 497 and 500 nm in DMF and DMSO, which corresponds to the π-π* transition. When the solvent polarity increased from DCM to DMF, Pyridine-NH_2 is stabilized by the greater polarity that is found in DMSO and DMF due to the strong hydrogen bond interactions. We also investigated the Pyridine-PTyr fluorescence properties in methanol, DMF and DMSO as shown in Figure 6(B). The Pyridine-PTyr fluorescence emission peaks were at located at 519, 496 and 505 nm in methanol, DMF and DMSO, respectively. The absorption and emission result show that Pyridine-NH_2 exhibits the solvatochromism effect, while Pyridine-PTyr did not show the solvatochromism effect. Figure 7 presents the fluorescence emission spectra of Pyridine-NO_2, Pyridine-NH_2 and Pyridine-PTyr in the solid state. Pyridine-NO_2 does not exhibit any emission peaks, while Pyridine-NH_2 shows two fluorescence emission peaks at 436 nm due to monomer emission and at 486 nm corresponding to the excimer emission. Interestingly, Pyridine-PTyr displays a very strong emission peak at 536 nm and a bathochromic shift as shown in Figure 7. Therefore, we carefully performed further experiments to prove these interesting phenomena and to report for the first time on the properties of the triphenyl pyridine functionalized-polytyrosine as AIE unit in the polymer centre (Pyridine-PTyr). In order to investigate the optical properties of Pyridine-NH_2 and Pyridine-PTyr with solvent molecules, The quantum yields (Φ_f) of Pyridine-NH_2 and Pyridine-PTyr in solution were measured by using quinine sulfate in 1 N H_2SO_4 (Φ_f = 0.55) as the standard. The quantum yields results are summarized in Table S1. In addition, quantum efficiency (Φ_f) of Pyridine-NH_2 and Pyridine-PTyr in solid state was 25.8 and 38.3 %, respectively. The values of fluorescence lifetime for Pyridine-NH_2 and Pyridine-PTyr in solid state were τ_1 = 0.14 ns and τ_1 = 0.13, τ_2 = 9.24 ns, respectively, based on Figure S5.

Aggregation-induced emission (AIE) phenomena

As mentioned above, most of organic emissive materials exhibit a high emission in solution but quenched emissions in concentrated solution and the aggregate (solid) state. This type of emission quenching is due to noncovalent intramolecular interactions such as π-π stacking and is known as aggregation-caused emission

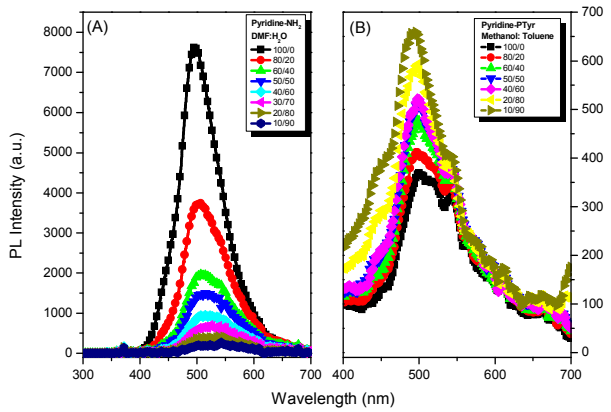

Figure 9: Photoluminescence spectra of (A) Pyridine-NH_2 in the DMF/water and (B) Pyridine-PTyr in the methanol/toluene with the concentration 1 x 10^{-4} M under 350 nm irradiation.

(ACQ). Our first question was whether our Pyridine-NH_2 (initiator) and Pyridine-PTyr (polymer) exhibit aggregation-induced emission (AIE) or not. We carefully investigated the AIE feature of Pyridine-NH_2 and Pyridine-PTyr using concentration effect and solvent pairs. Figure 8 shows the concentration effect of fluorescence emission of Pyridine-NH_2 and Pyridine-PTyr. Figure 8(A) shows that the emission intensity decreased by increasing the Pyridine-NH_2 concentration in DMF solution. The concentration-quenched emission is observed for Pyridine-NH_2 due to the intramolecular π-π interaction and formation of an excimer. Figure 8(B) shows the concentration effect on the emission behavior of Pyridine-PTyr. As shown in Figure 5(B), dilute solution of Pyridine-PTyr 10^{-5} M contain very small amount of fluorophore and it showed a very weak emission. However, the increasing of Pyridine-PTyr concentration from 10^{-4} to 10^{-2} M, the emission intensity gained a continuous increased in methanol solution. The concentration-enhanced emission observed for Pyridine-PTyr methanol solution which ascribed to the AIEE effect. Based on these rather interesting results, we strongly suggest that emission in Pyridine-NH_2 is transformed from aggregation-caused emission to AIEE by attachment to the rigid polytyrosine backbone. To further demonstrate the ACQ for Pyridine-NH_2, Pyridine-NH_2 behavior in solvent-non solvent DMF-water was studied as shown in Figure 9(A). In this study, we observe that in dilute Pyridine-NH_2 solution (10^{-4} M) in DMF emitted strongly at 520 nm. Furthermore, the fluorescence emission was decreased by increasing the water concentration and was up to 90% quenched. In this study, we did not select DMF as the good PTyr-Pyridine solvent to avoid the strong hydrogen bond interaction between the C=O group in DMF and the phenolic OH in polytyrosine. Interestingly, while preparing the stock solution of Pyridine-PTyr in methanol as the good solvent by varying the toluene (as the poor solvent) concentrations, we determined that the fluorescence emission were enhanced because of their aggregate nature. Hence, we performed the AIEE analysis. As shown in Figure 9(B), the PL intensities were enhanced by increasing the concentration of toluene (up to 90%). From these further experiments, we confirmed that the new PTyr-Pyridine fluorescent material exhibits the AIE while Pyridine-NH_2 is an ACQ material.

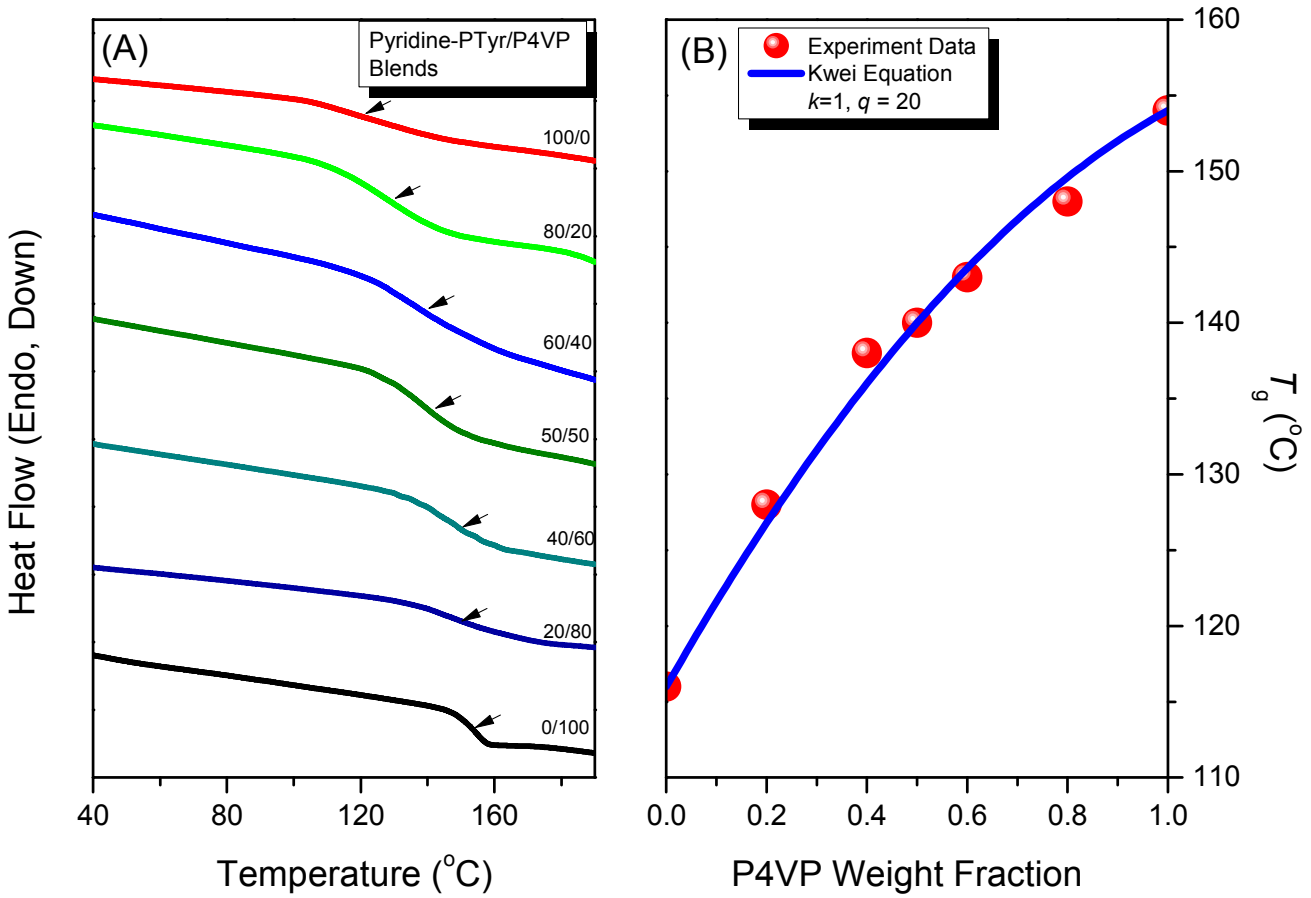

Figure 10: (A) DSC traces (third heating run) of Pyridine-PTyr /P4VP blends and (B) Plot Tg of Pyridine-PTyr with increasing P4VP contents.

Hydrogen Bonding Interaction between Pyridine-PTyr /P4VP Blends

(a) Thermal Analyses of Pyridine-PTyr /P4VP Blends

The DSC technique was used to perform the thermal analysis of Pyridine-PTyr in the pure state and their miscibility after blending with different weight ratios of poly(4-vinylpyridine) through mediated intermolecular hydrogen bonding in DMF solution as shown in Figure 10. Figure 10(A) reveals that the glass transition temperature of pure Pyridine-PTyr used in this study was only lower than that of the pure linear PTyr (155 °C);[21] this finding was attributed to the bowl-shaped corannulene ring and noncoplanar triphenylpyridine unit that increase the free volume and subsequently decrease the T_g behavior. Clearly, a single T_g behavior was found for PTyr-Pyridine/P4VP blends, indicating the total miscibility in this blend system. Moreover, in Figure 10(B), the glass transition temperatures for Pyridine-PTyr /P4VP blends increased with increasing P4VP content due to hydrogen bonding interactions between pairs of electrons on N atom in pyridine groups of P4VP and the phenolic OH of Pyridine-PTyr. Additionally, we obtained the values of k and q of 1 and 20, respectively, for Pyridine-PTyr/P4VP blends based on the Kwei equation.[33]The positive q value implies that inter-association interaction between Pyridine-PTyr/P4VP is stronger than self-association of Pyridine-PTyr. The conclusion from these results the Pyridine-PTyr/P4VP blend system shows that the random coils were separated.

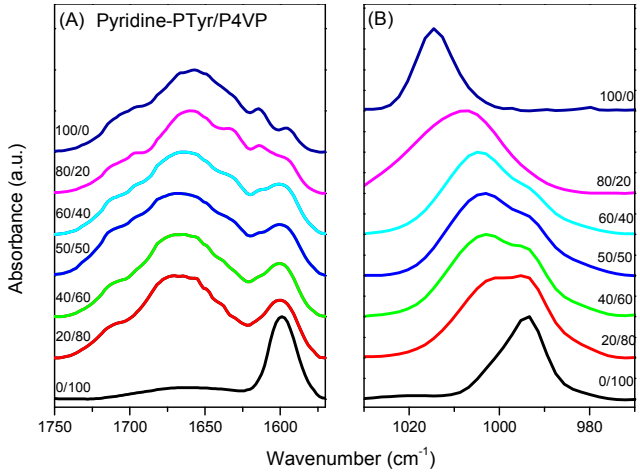

Figure 11: FTIR spectra recorded at ambient temperature, displaying the region between (A)1030 and 970 cm^{-1} (A) and region between (1750-1580 cm-1) (B) for PTyr-Pyridine/P4VP blends

(b) Conformation Transition and Hydrogen Bonding Interaction of Pyridine-PTyr/P4VP Blends in Bulk State

FTIR spectroscopy provides a simple, quick and facile method to investigate the non-covalent interactions between poly(4-vinylpyridine) and Pyridine-PTyr; we also studied the secondary structures conformation of Pyridine-PTyr/P4VP blends in solid state at room temperature. The hydrogen bonding between the

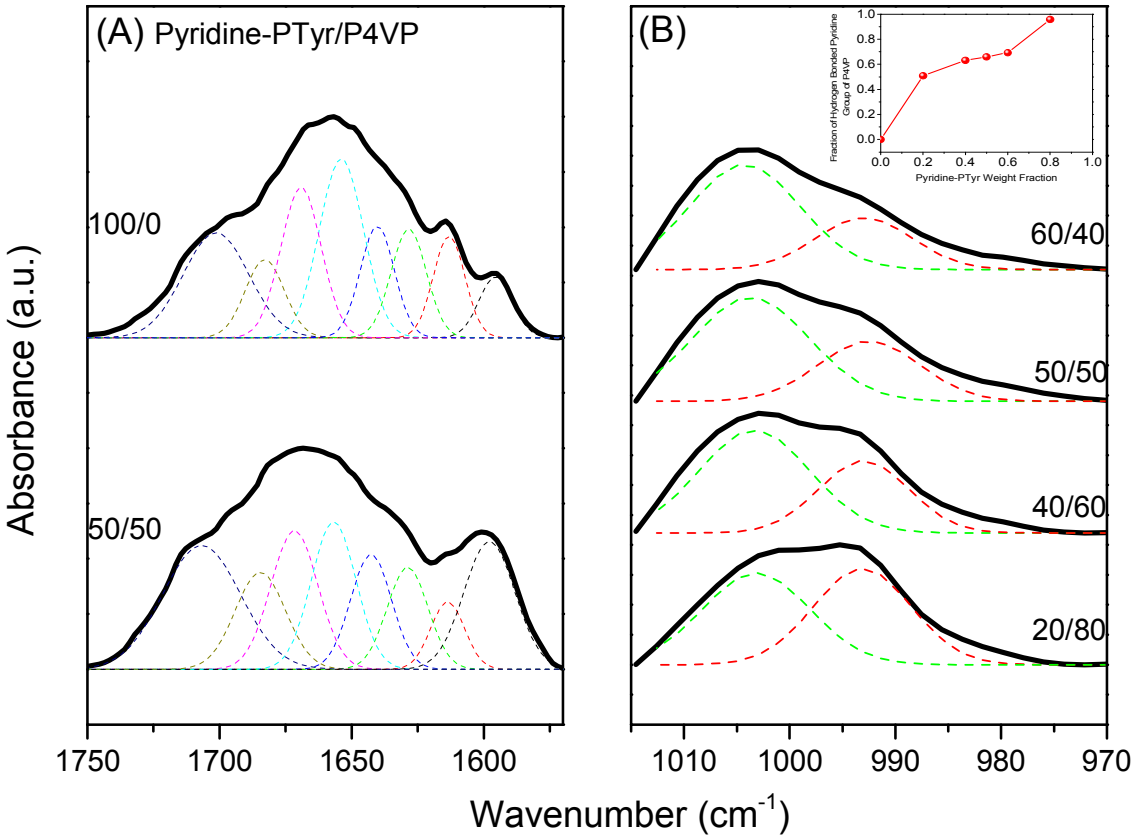

Figure 12: Curve fitting of the signals in the FTIR spectra of Pyridine-PTyr/P4VP blends of (A) amide I group and (B) pyridine group

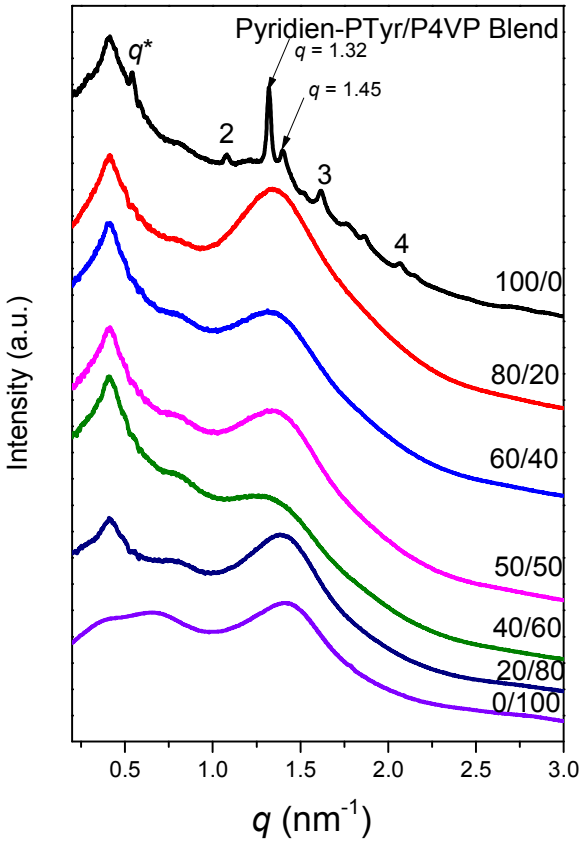

Figure 13: WAXD patterns of the Pyridine-PTyr/P4VP blends

pyridine ring and phenolic OH groups in Pyridine-PTyr was investigated by FTIR spectroscopy as shown in Figure 11. The hydrogen bond acceptance of P4VP can be monitored by observing the shifts of the pyridine ring modes at 993 cm^{-1},[34] as shown in Figure 11(B). Indeed, this finding clearly exhibits band shifts of the lowest wavenumber from 993 to 1005 cm^{-1};[35,36] it is possible to use two absorption peaks to analyze the specific interaction by subtracting the signal for pure Pyridine-PTyr at 1015 cm^{-1} based on the weight fraction of Pyridine-PTyr in these blends as shown in Figure 12(B). Clearly, the fraction of hydrogen-bonded Pyridyl groups increased with the increase of Pyridine-PTyr weight fraction as shown in the inset of Figure 12(B).

As mentioned in the introduction part, the secondary structures of polypeptide are strongly dependent on the degree of polymerization DP. For example, Pakula et al, reported that α-helical secondary structure of PBLG is favored at degree of polymerization >18.[37]As shown in Figure 12(A), in this study we observed major peaks for pure Pyridine-PTyr using the second-derivative technique: 1597 and 1615 cm^{-1} for the ring vibrations of tyrosine; 1655 cm^{-1} for the α-helical conformation; 1630 cm^{-1} for the β-sheet conformation; 1670 cm^{-1} for the β-turn conformation; and 1643, 1683, and 1700 cm^{-1} for the random coil conformation. Clearly, when it blended with 50 wt% ratio of P4VP, the secondary structures (α-helical and β-sheet) conformation was decreased and the fraction of random coil conformation was increased from 37.2% to 42.4%.

To further elucidate the changes in the secondary structures of the Pyridine-PTyr/P4VP blends, WAXD experiments were performed at room temperature as provided in Figure 13. In Figure 13, the Bragg's diffraction pattern provided the presence of β-sheet secondary structures for pure Pyridine-PTyr (DP = 10).

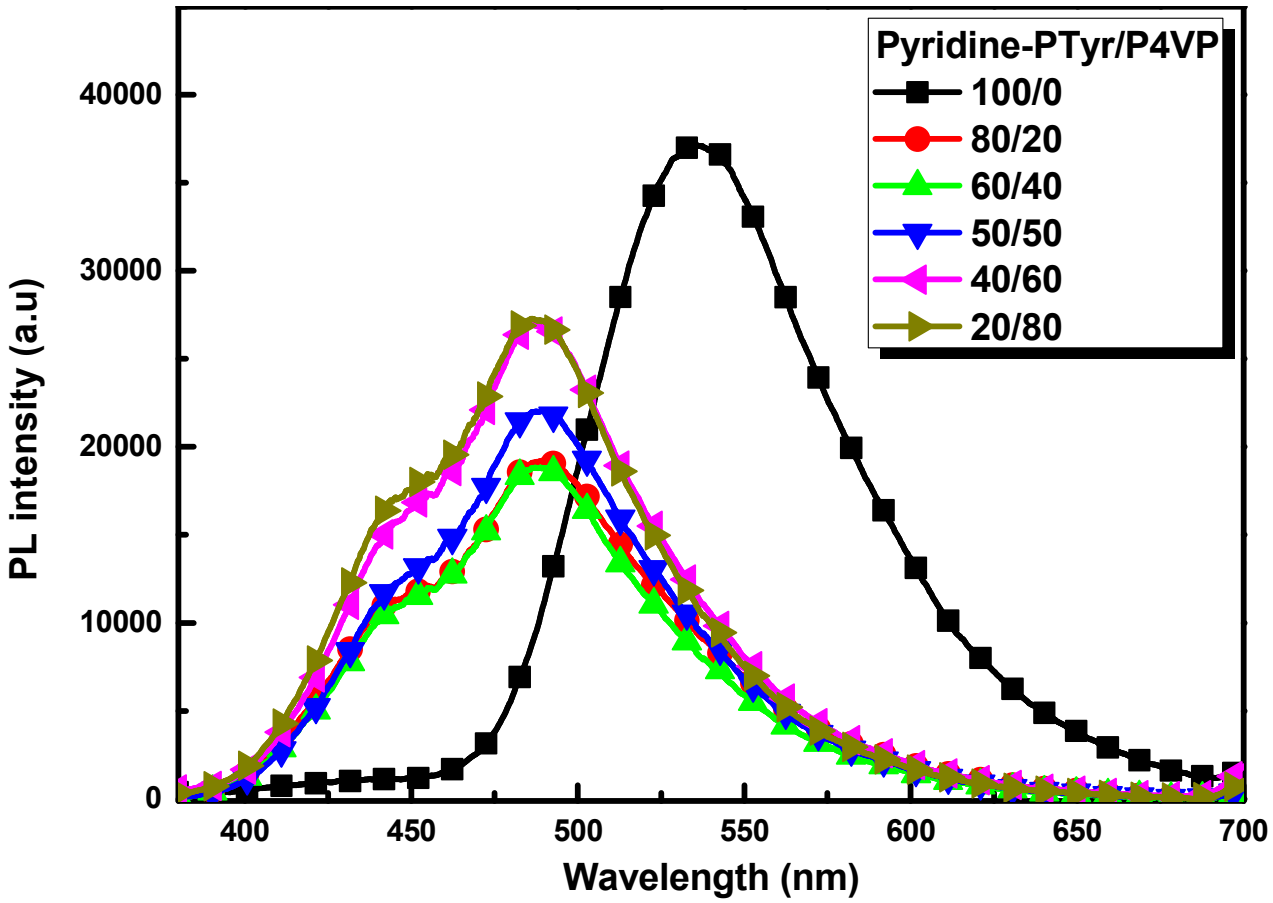

Figure 14: Photoluminescence spectroscopy of Pyridine-PTyr/P4VP blends in solid state under 350 nm irradiation.

For more details, we can observe the signature of the first such structure at q=0.54 (d = 1.15 nm), corresponding to the distance between the backbones in the antiparallel β-pleated sheet structure. the diffraction peak centered at q=1.32 (corresponding to d = 0.475 nm) is observed, indicating the intermolecular distance between adjacent peptide chains within one lamella.[38] Clearly, the secondary structure of β-sheet conformation has disappeared, and as shown the diffraction patterns of Pyridine-PTyr become a broad amorphous halo after increasing the P4VP content in the Pyridine-PTyr/P4VP blend system.[21]

(c) Emission properties of Pyridine-PTyr /P4VP blends in solid state

As mentioned above, Pyridine-PTyr showed an aggregation-induced emission phenomena and notably high fluorescence emission intensity. Interestingly, after blending with P4VP (20, 40, 50 wt %), the Pyridine-PTyr emission intensity decreased and hypsochromic shift from 536 to 489 nm was observed (Figure 14); this was attributed to the hydrogen bonding interaction between P4VP and phenolic OH groups of PTyr and the release of the restricted intramolecular rotation of the triphenyl pyridine unit in the center of the polymer. When the P4VP content increased (up to 60, 80 wt %), the fluorescence intensities increased gradually because of the restricted intramolecular rotation of triphenyl pyridine unit, while the PL emission peak still exhibited the hypsochromic shift. We also measured quantum efficiency (Φ_f) in solid state and the values were 38.3, 32.8, 32.8, 34.8 and 35.4 for 20, 40, 50, and 60 wt% of P4VP in Pyridine-PTyr/P4VP blend system. We also measured temperature-dependent fluorescence of Pyridine-PTyr/P4VP blend (40/60) to investigate the role of hydrogen bonding interaction in this study as shown in Figure S6. As shown in Figure S6, the emission intensity of Pyridine-PTyr/P4VP is still remained without any changing at temperature from 25 to 60 ^{o}C which attributed to restrict intramolecular rotation of the blend. However, decreasing emission intensity of Pyridine-PTyr/P4VP was observed at temperature from 80 to 160 ^{o}C because of release intramolecular rotation and dissociation of intermolecular hydrogen bonding between phenolic hydroxyl group in polytyrosine chain and pyridine ring in P4VP.

Conclusions

In this report, the synthetic route of Pyridine-PTyr homopolymer through ROP of L-tyrosine-N-carboxyanhydride using pyridine-NH_2 as initiator with controlled PDI was described and tested. We carefully confirmed its chemical structure using FTIR, ^{1}H and ^{13}C NMR, and MALDI-TOF mass spectroscopies. Interestingly, the PL results revealed that while Pyridine-NH_2 was an ACQ material, it became a strongly AIE material after attachment to the rigid-rod polytyrosine due to the restriction of intramolecular rotation (RIR) mechanism. DSC analysis revealed that the glass transition temperature of Pyridine-PTyr (120 ^{o}C) was lower than that of the pure linear polytyrosine (155 ^{o}C) due to its bowl-shaped corannulene ring and noncoplanar triphenylpyridine unit. We determined that the emission intensity of Pyridine-PTyr was decreased and a hypsochromic shift from 536 to 489 nm was observed due to the release of the restricted intramolecular rotation of triphenyl pyridine unit in the center of the polymer caused by the intermolecular hydrogen bonding of PTyr with P4VP; this conclusion was based on the results of IR spectroscopy, while the separated random coils behavior of the

Pyridine-PTyr chains was deduced from the analysis of the wide-angle X-ray diffraction.

Acknowledgments

This study was supported financially by the Ministry of Science and Technology, Taiwan under contracts MOST103-2221-E-110-079-MY3 and MOST102-2221-E-110-008-MY3.

Electronic supplementary information (ESI) available:

Experimental detail of DSC, NMR, MS, GPC and fluorescence lifetime of Pyridine-NH_2 and Pyridine-PTyr behaviour are available.

Reference

1 S. N. S. Alconel, S. A. Baas and D. H. Maynard, *Polym. Chem*., 2011, **2**, 1442-1448.
2 A. H. Gauthier and A. H. Klok, *Chem. Commun*., 2008, 2591-2611.
3 Y. Chen, H. X. Pang and M. C. Dong, *Adv. Funct. Mater*., 2010, **20**, 579-586.
4 M. S. Peng, Y. Chen, C. Hua and M. C. Dong, *Macromolecules*, 2009, **42**, 104-113.
5 T. J. Deming, *Adv. Mater*., 1997, **9**, 299-311.
6 X. Zhang, J. Li, W. Li and A. Zhang, *Biomacromolecules*, 2007, **8**, 3557-3567.
7 H. R. Kricheldorf, *Angew. Chem. Int. Ed.*, 2006, **45**, 5752-5784.
8 T. J. Deming, *Prog. Polym. Sci*., 2007, **32**, 858-875.
9 P. Papadopoulous, G. Floudas, A. H. Klok, I. Schnell and T. Pakula, *Biomacromolecules*, 2004, **5**, 81-91.
10 N. Hadjichristidis, H. Iatrou, M. Pitsikalis and G. Sakellariou, *Chem. Rev*., 2009, **109**, 5528-5578.
11 C. He, X. Zhuang, Z. Tang, H. Tian and X. Chen, *Adv. Healthcare Mater*., 2012, **1**, 48-78.
12 H. Tang and D. Zhaung, *Biomacromolecules*, 2010, **11**, 1585-1592.
13 J. R. Kramer and T. J. Deming, *J. Am. Chem. Soc*., 2012, **132**, 15068-15071.
14 C. Chen. Z. Wang and Z. Li. *Biomacromolecules*, 2011, **12**, 2859-2863.
15 X. Fu, Y. Shen, W. Fu and Z. Li, *Macromolecules*, 2013, **46**, 3753-3760.
16 Y. C. Lin, and S. W. Kuo, *Polym. Chem.*, 2012, **3**, 162-171.
17 Y. C. Lin, and S. W. Kuo, *Polym. Chem.*, 2012, **3**, 882-891.
18 Y. C. Lin, P. I. Wang, and S. W. Kuo, *Soft Matter*, 2012, **8**, 9676-9684.
19 S. W. Kuo and C. J. Chen, *Macromolecules*, 2011, **44**, 7315-7326.
20 S. W. Kuo and C. J. Chen, *Macromolecules*, 2012, **45**, 2442-2452.
21 Y. S. Lu, Y. C. Lin and S. W. Kuo, *Macromolecules*, 2012, **45**, 6547-6556.
22 F. Y. Yan, M. Wang, D. L. Cao, N. Yang, Y. Fu, L. Chen and L. G. Chen, *Dyes Pigm*., 2013, **98**, 42-50.
23 M. Xavier, P. Fabien, L. D. Thilo, D. Maxime, B. P. Marcel, A. A. Paul and W. Shimon, *Single Mol*., 2001, **2**, 261-276.
24 S. Chenais and S. Forget, *Polym. Int*., 2012, **61**, 390-406.
25 S. A. Jenekhe and J. A. Osaheni, *Science*, 1994, **265**, 765-768.
26 (a) R. H. Friend, R. W. Gymer, A. B. Holmes, J. H. Burroughes, R. N. Marks and C. Taliani, Nature., 1999, 397, 121-128. (b) K. Y. Pu and B. Liu, *Adv. Funct. Mater*., 2009, **19**, 277-284. (c) X. Zhang, M. Cui, R. Zhou, C. Chen and G. Zhang, *Macromol. Rapid Commun*., 2014, **35**, 566-573. (d) G. Zhang, G. M. Palmer, M. W. Dewhirst and C. L. Fraser, *Nature Mater*., 2009, **8**, 747-751. (d) Y. Cao, W. Xi, L. Wang, H. Wang, L. Kong, H. Zhou, J. Wu and Y. Tian, *RSC Adv.*, 2014, **4**, 24649-24652. (e) M. S. Zakerhamidi, A. Ghanadzadeh and M. Moghadam, *Chem. Sci.*, 2012, **1**, 1-8. (f) G. Zhang, M. P. Aldred, W. L. Gong, C. Li and M. Q. Zhu, *Chem. Commun.*, 2012, **48**, 7711-7713.
27 (a) J. Luo, Z. Xie, J. W. Y. Lam, L. Cheng, H. Chen, C. Qiu, H. S. Kwok, X. Zhan, Y. Liu, D. Zhu and B. Z. Tang, *Chem. Commun*., 2001, 1740-1741. (b) Z. Zhao, S. Chen, J. W. Y. Lam, P. Lu, Y. Zhong, K. S. Wong, H. S. Kwok and B. Z. Tang, *Chem. Commun*., 2010, **46**, 2221-2223. (c) J. Liu, Y. Zhong, J. W. Y. Lam, P. Lu, Y. Hong, Y. Yu, Y. Yue, M. Faisal, H. H. Y. Sung, I. D. Williams, K. S. Wong and B. Z. Tang, *Macromolecules*, 2010, **43**, 4921-4936. (d) R. H. Chien, C. T. Lai and J. L. Hong, *Macromol. Chem. Phys*., 2012, **213**, 666-677.
28 S. T. Li, Y. C. Lin, S. W. Kuo, W. T. Chuang and J. L. Hong, *Polym. Chem*., 2012, **3**, 2393-2402.
29 K. Y. Shih, Y. C. Lin, T. S. Hsiao, S. L. Deng, S. W. Kuo and J. L. Hong, *Polym. Chem*., 2014, **5**, 5765-5774.
30 C. H. Lin, Y. S. Shih, M. W. Wang, C. Y. Tseng, T. Y. Juang and C. F. Wang, *RSC. Adv*., 2014, **4**, 8692-8698.
31 R. L. Frank and R. P. Seven, *J. Am. Chem. Soc*., 1949, **71**, 2629-2635.
32 G. J. M. Habraken, M. Peeters, C. H. J. T. Dietz, C. E. Koning and A. Heise, *Polym. Chem*., 2010, **1**, 514-524.
33 T. K. Kwei, J. *Polym. Sci.: Polym. Lett. Ed*., 1984, **22**, 307-313.
34 S. W. Kuo, P. H. Tung and F. C. Chang, *Macromolecules*, 2006, **39**, 9388-9395.
35 J. Y. Lee, P. C. Painter and M. M. Coleman, *Macromolecules*, 1988, **21**, 954-960.
36 S. W. Kuo, C. L. Lin, and F. C. Chang, *Polymer*, 2002, **43**, 3943-3949.
37 P. Papadopoulous, G. Floudas, A. H. Klok, I. Schnell and T. Pakula, *Biomacromolecules*, 2004, **5**, 81-91.
38 H. E. Auer, and R. P. Mcknight, *Biochem.,* 1978, **14**, 2793-2798.

Graphic Abstract

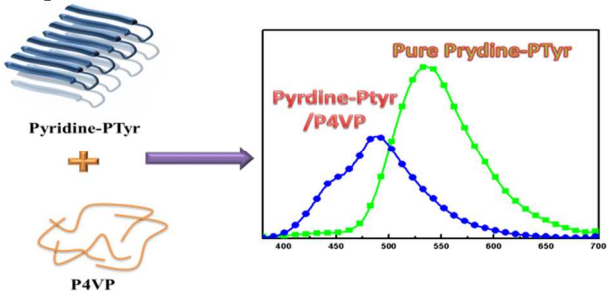

The emission intensity of Pyridine-PTyr was decreased after blending with P4VP and hypsochromic shift from 536 to 489 nm due to the release of the restricted intramolecular rotation of triphenyl pyridine unit in the center of the polymer